Discovery of biased orientations of human DNA motif sequences affecting enhancer-promoter interactions and transcription of genes

Naoki Osato[1*]

[1]Department of Bioinformatic Engineering, Graduate School of Information Science and Technology, Osaka University, Osaka 565-0871, Japan

[*]Corresponding author

E-mail address: naokiosato11@gmail.com, nosato@ist.osaka-u.ac.jp

Abstract

Chromatin interactions have important roles for enhancer-promoter interactions (EPI) and regulating the transcription of genes. CTCF and cohesin proteins are located at the anchors of chromatin interactions, forming their loop structures. CTCF has insulator function limiting the activity of enhancers into the loops. DNA binding sequences of CTCF indicate their orientation bias at chromatin interaction anchors – forward-reverse (FR) orientation is frequently observed. DNA binding sequences of CTCF were found in open chromatin regions at about 40% - 80% of chromatin interaction anchors in Hi-C and in situ Hi-C experimental data. Though the number of chromatin interactions was about seventy thousand in Hi-C at 50kb resolution, about twenty millions of chromatin interactions were recently identified by HiChIP at 5kb resolution. It has been reported that long range of chromatin interactions tends to include less CTCF at their anchors. It is still unclear what proteins are associated with chromatin interactions.

To find DNA binding motif sequences of transcription factors (TF), such as CTCF, and repeat DNA sequences affecting the interaction between enhancers and promoters of genes and their expression, first I predicted TF bound in enhancers and promoters using DNA motif sequences of TF and experimental data of open chromatin regions in monocytes and other cell types, which were obtained from public and commercial databases. Second, transcriptional target genes of each TF were predicted based on enhancer-promoter association (EPA). EPA was shortened at the genomic locations of FR or reverse-forward (RF) orientation of DNA motif sequence of a TF,

which were supposed to be at chromatin interaction anchors and acted as insulator sites like CTCF. Then, the expression levels of the transcriptional target genes predicted based on the EPA were compared with those predicted from only promoters.

Total 229 biased orientations of DNA motifs (130 FR and 128 RF orientations, the reverse complement sequences of some DNA motifs were also registered in databases, so the total number was smaller than the number of FR and RF) affected the expression level of putative transcriptional target genes significantly in $CD14^+$ monocytes of four people in common. The same analysis was conducted in $CD4^+$ T cells of four people. DNA motif sequences of CTCF, cohesin and other transcription factors involved in chromatin interactions were found to be a biased orientation. Transposon sequences, which are known to be involved in insulators and enhancers, showed a biased orientation. The biased orientations of DNA motif sequences tended to be co-localized in the same open chromatin regions. Moreover, for 51 - 204 of FR and RF orientations of DNA motif sequences in $CD4^+$ T cells, EPI predicted from EPA that were shortened at the genomic locations of the biased orientation of DNA motif sequence were overlapped with chromatin interaction data significantly more than other types of EPAs.

Keywords: transcriptional target genes, gene expression, transcription factors, enhancer, enhancer-promoter interactions, chromatin interactions, CTCF, cohesin, open chromatin regions, co-location of transcription factors, homodimer, heterodimer, complex

55

56 **Background**

57 Chromatin interactions have important roles for enhancer-promoter interactions
58 (EPI) and regulating the transcription of genes. CTCF and cohesin proteins are located
59 at the anchors of chromatin interactions, forming their loop structures. CTCF has
60 insulator function limiting the activity of enhancers into the loops (Fig. 1A). DNA
61 binding sequences of CTCF indicate their orientation bias at chromatin interaction
62 anchors – forward-reverse (FR) orientation is frequently observed (de Wit et al. 2015;
63 Guo et al. 2015). About 40% - 80% of chromatin interaction anchors of Hi-C and in situ
64 Hi-C experiments include DNA binding motif sequences of CTCF. Though the number
65 of chromatin interactions was about seventy thousand in Hi-C at 50kb resolution
66 (Javierre et al. 2016), about twenty millions of chromatin interactions were recently
67 identified by HiChIP at 5kb resolution (Mumbach et al. 2017). However, it has been
68 reported that long range of chromatin interactions tends to include less CTCF at their
69 anchors (Jeong et al. 2017). Other DNA binding proteins such as ZNF143, YY1, and
70 SMARCA4 (BRG1) are found to be associated with chromatin interactions and EPI
71 (Bailey et al. 2015; Barutcu et al. 2016; Weintraub et al. 2017). CTCF, cohesin,
72 ZNF143, YY1 and SMARCA4 have other biological functions as well as chromatin
73 interactions and EPI. The DNA binding motif sequences of the transcription factors
74 (TF) are found in open chromatin regions near transcriptional start sites (TSS) as well as
75 chromatin interaction anchors.

76 DNA binding motif sequence of ZNF143 was enriched at both chromatin

77 interaction anchors. ZNF143's correlation with the CTCF-cohesin cluster relies on its
78 weakest binding sites, found primarily at distal regulatory elements defined by the
79 'CTCF-rich' chromatin state. The strongest ZNF143-binding sites map to promoters
80 bound by RNA polymerase II (POL2) and other promoter-associated factors, such as the
81 TATA-binding protein (TBP) and the TBP-associated protein, together forming a
82 'promoter' cluster (Bailey et al. 2015).

83 DNA binding motif sequence of YY1 does not seem to be enriched at both
84 chromatin interaction anchors (Z-score < 2), whereas DNA binding motif sequence of
85 ZNF143 is significantly enriched (Z-score > 7; Bailey et al. 2015 Figure 2a). In the
86 analysis of YY1, to identify a protein factor that might contribute to EPI, (Ji et al. 2015)
87 performed chromatin immune precipitation with mass spectrometry (ChIP-MS), using
88 antibodies directed toward histones with modifications characteristic of enhancer and
89 promoter chromatin (H3K27ac and H3K4me3, respectively). Of 26 transcription factors
90 that occupy both enhancers and promoters, four are essential based on a CRISPR
91 cell-essentiality screen and two (CTCF, YY1) are expressed in >90% of tissues
92 examined (Weintraub et al. 2017). These analyses started from the analysis of histone
93 modifications of enhancer and promoter marks rather than chromatin interactions. Other
94 protein factors associated with chromatin interactions may be found from other
95 researches.

96 As computational approaches, machine-learning analyses to predict chromatin
97 interactions have been proposed (Schreiber et al. 2017; Zhang et al. 2017). However,
98 they were not intended to find DNA motif sequences of TF affecting chromatin

99 interactions, EPI, and the expression level of transcriptional target genes, which were
100 examined in this study.

101 DNA binding proteins involved in chromatin interactions are supposed to affect
102 the transcription of genes in the loops formed by chromatin interactions. In my previous
103 analysis, the expression level of human putative transcriptional target genes was
104 affected, according to the criteria of enhancer-promoter association (EPA) (Fig. 1B;
105 (Osato 2018)). EPI were predicted based on EPA shortened at the genomic locations of
106 FR orientation of CTCF binding sites, and transcriptional target genes of each TF bound
107 in enhancers and promoters were predicted based on the EPI. The EPA affected the
108 expression levels of putative transcriptional target genes the most among three types of
109 EPAs, compared with the expression levels of transcriptional target genes predicted
110 from only promoters (Fig. 2). The expression levels tended to be increased in
111 monocytes and $CD4^+$ T cells, implying that enhancers activated the transcription of
112 genes, and decreased in ES and iPS cells, implying that enhancers repressed the
113 transcription of genes. These analyses suggested that enhancers affected the
114 transcription of genes significantly, when EPI were predicted properly. Other DNA
115 binding proteins involved in chromatin interactions, as well as CTCF, may locate at
116 chromatin interaction anchors with a pair of biased orientation of DNA binding motif
117 sequences, affecting the expression level of putative transcriptional target genes in the
118 loops formed by the chromatin interactions. As experimental issues of the analyses of
119 chromatin interactions, chromatin interaction data are changed, according to
120 experimental techniques, depth of DNA sequencing, and even replication sets of the

121 same cell type. Chromatin interaction data may not be saturated enough to cover all
122 chromatin interactions. Supposing these characters of DNA binding proteins associated
123 with chromatin interactions and avoiding experimental issues of the analyses of
124 chromatin interactions, here I searched for DNA motif sequences of TF and repeat DNA
125 sequences, affecting EPI and the expression level of putative transcriptional target genes
126 in $CD14^+$ monocytes and $CD4^+$ T cells of four people without using chromatin
127 interaction data. Then, putative EPI were compared with chromatin interaction data.
128

129 ## Results

130 **Search for biased orientation of DNA motif sequences**

131 Transcription factor binding sites (TFBS) were predicted using open chromatin
132 regions and DNA motif sequences of transcription factors (TF) collected from various
133 databases and journal papers (see Methods). Transcriptional target genes were predicted
134 using TFBS in promoters and enhancer-promoter association (EPA) shortened at the
135 genomic locations of DNA binding motif sequence of a TF acting as insulator such as
136 CTCF and cohesin (RAD21 and SMC3) (Fig. 1B). To find DNA motif sequences of TF
137 acting as insulator, other than CTCF and cohesin, and repeat DNA sequences affecting
138 the expression level of genes, EPI were predicted based on EPA shortened at the
139 genomic locations of the DNA motif sequence of a TF or a repeat DNA sequence, and
140 transcriptional target genes of each TF bound in enhancers and promoters were
141 predicted based on the EPI. The expression levels of the putative transcriptional target
142 genes were compared with those predicted from promoters using Mann Whiteney U test,

143 two-sided (p-value < 0.05) (Fig. 2A). The number of TF showing a significant
144 difference of expression level of their putative transcriptional target genes was counted.
145 To examine whether the orientation of a DNA motif sequence, which is supposed to act
146 as insulator sites and shorten EPA, affected the number of TF showing a significant
147 difference of expression level of their putative transcriptional target genes, the number
148 of the TF was compared among forward-reverse (FR), reverse-forward (RF), and any
149 orientation (i.e. without considering orientation) of a DNA motif sequence shortening
150 EPA, using Fisher's exact test (p-value < 0.05). To avoid missing DNA motif sequences
151 showing a relatively weak statistical significance by multiple testing correction, the
152 above analyses were conducted using monocytes of four people independently, and
153 DNA motif sequences found in monocytes of four people in common were selected.
154 Total 229 of biased (130 FR and 128 RF) orientation of DNA binding motif sequences
155 of TF were found in monocytes of four people in common, whereas only 11 any
156 orientation of DNA binding motif sequence was found in monocytes of four people in
157 common (Fig. 2B; Table 1; Supplemental Table S1). FR orientation of DNA motif
158 sequences included CTCF, cohesin (RAD21), and YY1, which are associated with
159 chromatin interactions and EPI. NFI (Nuclear factor-1) has been reported to have
160 enhancer-blocking activity (Gaussin et al. 2012), and NFI showed a biased orientation
161 in monocytes and $CD4^+$ T cells.

162 The same analysis was conducted using DNase-seq data of $CD4^+$ T cells of four
163 people. Total 211 of biased (120 FR and 122 RF) orientation of DNA binding motif
164 sequences of TF were found in T cells of four people in common, whereas only 15 any

165 orientation (i.e. without considering orientation) of DNA binding motif sequences were
166 found in T cells of four people in common (Supplemental Fig. S1 and Supplemental
167 Table S2). Biased orientation of DNA motif sequences in T cells included CTCF,
168 cohesin (RAD21 and SMC3), YY1 and SMARC. SMARCA4 (BRG1) is associated
169 with topologically associated domain (TAD), which is higher-order chromatin
170 organization. The DNA binding motif sequence of SMARCA4 was not registered in the
171 databases used in this study. FR orientation of DNA motif sequences included
172 SMARCC2, a member of the same SWI/SNF family of proteins as SMARCA4. Biased
173 orientation of DNA motif sequences included JUNDM2 (JDP2), which is involved in
174 histone-chaperone activity, promoting nucleosome, and inhibition of histone acetylation
175 (Jin et al. 2006). JDP2 forms a homodimer or heterodimer with various TF
176 (https://en.wikipedia.org/wiki/Jun_dimerization_protein). Between 229 and 211, 69 of
177 biased orientation of DNA binding motif sequences of TF were found in both
178 monocytes and T cells in common (Supplemental Table S5). For each orientation, 42
179 FR and 36 RF orientations of DNA binding motif sequences of TF were found in both
180 monocytes and T cells in common. Without considering the difference of orientation of
181 DNA binding motif sequences, 88 of biased orientation of DNA binding motif
182 sequences of TF were found in both monocytes and T cells. As a reason for the increase
183 of the number (88) from 69, a TF or an isoform of the same TF may bind to a different
184 DNA binding motif sequence according to cell types and/or in the same cell type. About
185 50% or more of alternative splicing isoforms are differently expressed among tissues,
186 indicating that most alternative splicing is subject to tissue-specific regulation (Wang et

187 al. 2008) (Chen and Manley 2009) (Das et al. 2007). The same TF has several DNA
188 binding motif sequences and in some cases one of the motif sequences is almost the
189 same as the reverse complement sequence of another motif sequence of the same TF.
190 For example, RAD21 had both FR and RF orientations of DNA motif sequences, but
191 the number of the FR orientation of DNA motif sequence was relatively small in the
192 genome, and the RF orientation of DNA motif sequence was frequently observed and
193 co-localized with CTCF. I previously found that a complex of TF would bind to a
194 slightly different DNA binding motif sequence from the combination of DNA binding
195 motif sequences of TF composing the complex in *C. elegans* (Tabuchi et al. 2011).
196 From another viewpoint of this study, the expression level of putative transcription
197 target genes of some TF would be different, depending on the genomic locations
198 (enhancers or promoters) of DNA binding motif sequences of the TF in monocytes and
199 T cells of four people.

200 Moreover, using open chromatin regions overlapped with H3K27ac histone
201 modification marks known as enhancer and promoter marks, the same analyses were
202 performed in monocytes and T cells. H3K27ac histone modification marks were used in
203 the analysis of EPI, but were not used in the analysis of TF as insulator like CTCF and
204 cohesin in this study, since new biased orientation of DNA motif sequences were found
205 in this criterion. When H3K27ac histone modification marks were used in the analysis
206 of TF as insulator like CTCF and cohesin, the number of biased orientation of DNA
207 motif sequences was decreased. Total 188 of biased (105 FR and 107 RF) orientations
208 of DNA binding motif sequences of TF were found in monocytes of four people in

209 common, whereas only nine any orientation of DNA binding motif sequence was found
210 (Supplemental Table S3). Though the number of biased orientations of DNA motif
211 sequences was reduced, CTCF, RAD21, SMC3, and YY1 were found. For T cells using
212 H3K27ac histone modification marks, total 178 of biased (108 FR and 96 RF)
213 orientation of DNA binding motif sequences of TF were found in T cells of four people
214 in common, whereas only 15 any orientation of DNA binding motif sequences were
215 found (Supplemental Table S4). Though the number of biased orientations of DNA
216 motif sequences was reduced, CTCF, RAD21, SMC3, and YY1 were found. As
217 summary of the results with and without H3K27ac histone modification marks, total
218 289 of biased (165 FR and 166 RF) orientation of DNA motif sequences were found in
219 monocytes of four people in common. Total 262 of biased (154 FR and 151 RF)
220 orientations of DNA motif sequences were found in T cells of four people in common.
221 Total number of these results in monocytes and T cells was 433 biased (262 FR and 264
222 RF) orientations of DNA motif sequences. Biased orientations of DNA motif sequences
223 found in both monocytes and T cells were listed in Supplemental Table S5.

224 Instead of DNA binding motif sequences of TF, repeat DNA sequences were also
225 examined. The expression levels of transcriptional target genes of each TF predicted
226 based on EPA that were shortened at the genomic locations of a repeat DNA sequence
227 were compared with those predicted from promoters. Three RF orientation of repeat
228 DNA sequences showed a significant difference of expression level of putative
229 transcriptional target genes in monocytes of four people in common (Table 2). The
230 same as $CD14^+$ monocytes, biased orientations of repeat DNA sequences were

231 examined in $CD4^+$ T cells. Two FR and one RF orientations of repeat DNA sequences
232 showed a significant difference of expression level of putative transcriptional target
233 genes in T cells of four people in common (Supplemental Table S6). MIRc was also
234 found in the analysis using open chromatin regions overlapped with H3K27ac histone
235 modification marks, which are enhancer and promoter marks. MIR and other transposon
236 sequences are known to act as insulators and enhancers (Bejerano et al. 2006; Rebollo et
237 al. 2012; de Souza et al. 2013; Jjingo et al. 2014; Wang et al. 2015).
238
239 **Co-location of biased orientations of DNA motif sequences**
240 To examine the association of 229 biased (FR and RF) orientations of DNA
241 binding motif sequences of TF, co-location of the DNA binding motif sequences in
242 open chromatin regions was analyzed in monocytes. The number of open chromatin
243 regions with the same pairs of DNA binding motif sequences was counted, and when
244 the pairs of DNA binding motif sequences were enriched with statistical significance
245 (Fisher's exact test, p-value $< 1.0 \times 10^{-9}$), they were listed (Table 3; Supplemental
246 Table S7). As already known, CTCF was found with cohesin RAD21 (Table 3). Top 30
247 pairs of FR and RF orientations of DNA motifs co-occupied in the same open chromatin
248 regions were shown (Table 3). Total number of pairs of DNA motifs was 261,
249 consisting of 148 unique DNA motifs, when the pair of DNA motifs was observed in
250 more than 60% of the number of open chromatin regions with the DNA motifs. Biased
251 orientations of DNA binding motif sequences of TF tended to be co-localized in the
252 same open chromatin regions.

253 To examine the association of 211 biased orientations of DNA binding motif
254 sequences of TF in $CD4^+$ T cells, co-location of the DNA binding motif sequences in
255 open chromatin regions was analyzed. Top 30 pairs of FR and RF orientations of DNA
256 motifs co-occupied in the same open chromatin regions were shown (Supplemental
257 Table S8). Total number of pairs of DNA motifs was 400, consisting of 141 unique
258 DNA motifs, when the pair of DNA motifs was observed in more than 60% of the
259 number of open chromatin regions with the DNA motifs (Fisher's exact test, *p*-value <
260 1.0×10^{-9}). Among them, 21 pairs of DNA motif sequences including a pair of CTCF,
261 and RAD21 in T cells were found in monocytes in common (Supplemental Table S8).
262 In both monocytes and $CD4^+$ T cells, some pairs of DNA motifs including CTCF
263 and RAD21 were found to be perfectly co-localized in the same open chromatin regions.
264 Almost all genomic positions of a DNA motif were located with genomic positions of
265 another DNA motif in the same open chromatin regions. This would be due to the strict
266 criteria of the search for DNA binding motif sequences of TF to reduce false prediction
267 of DNA binding sites of TF. Moreover, the number of pairs of DNA motif sequences
268 found in both monocytes and $CD4^+$ T cells in common was increased, compared with
269 general DNA motif searches using position weight matrix and allowing substitutions of
270 DNA sequences during motif searches. The score (*p*-value) of CTCF was relatively high
271 (50.54), but the score of RAD21 was lower (23.98) (Table 1). Almost all DNA binding
272 sequences of CTCF were co-localized with those of RAD21. However, some DNA
273 binding sequences of RAD21 were located in other genomic regions, which may not be
274 associated with chromatin interactions and biased orientations of the DNA motif

275 sequences. This might decrease the score of RAD21, compared with CTCF.

276

277 **Comparison with chromatin interaction data**

278 To examine whether the biased orientations of DNA motif sequences is
279 associated with chromatin interactions, enhancer-promoter interactions (EPI) predicted
280 based on enhancer-promoter associations (EPA) were compared with chromatin
281 interaction data. Due to the resolution of Hi-C experimental data available for this study
282 (50kb), HiChIP chromatin interaction data for $CD4^+$ T cells were used (Mumbach et al.
283 2017). EPI predicted based on EPA were compared with three replications (B2T1,
284 B2T2, and B3T1) of HiChIP chromatin interaction data in $CD4^+$ T cells respectively.
285 The resolutions of HiChIP chromatin interaction data and EPI were adjusted to 5kb. EPI
286 were predicted based on three types of EPA: (i) EPA shortened at the genomic locations
287 of FR or RF orientation of DNA motif sequence of a TF, (ii) EPA shortened at the
288 genomic locations of DNA motif sequence of a TF acting as insulator sites such as
289 CTCF without considering their orientation, and (iii) EPA without being shortened by
290 the genomic locations of a DNA motif sequence. EPI were predicted based on the three
291 types of EPA using top 60% expression level of all transcripts (genes) excluding
292 transcripts not expressed in T cells. The criteria of the analysis were determined to
293 include known DNA motif sequences involved in chromatin interactions such as CTCF
294 and cohesin in the result. EPA (i) showed the highest ratio of EPI overlapped with
295 chromatin interactions (HiChIP) using DNA binding motif sequences of CTCF and
296 cohesin (RAD21 and SMC3), compared with the other two types of EPA (ii) and (iii) (*n*

297 = 4, binomial test, two-sided, 95% confidence interval) (Supplemental Fig. S2). Total
298 51 biased orientation (33 FR and 23 RF) of DNA motif sequences, which included
299 CTCF, cohesin (RAD21 and SMC3), SMARCC1, and NFI in three replications (B2T1,
300 B2T2, and B3T1) showed a significantly higher ratio of EPI overlapped with HiChIP
301 chromatin interactions (more than 1,000 counts for each interaction) than the other types
302 of EPAs in T cells (Table 4). When comparing EPI predicted based on only EPA (i) and
303 (iii) with the chromatin interactions, total 204 biased orientation (116 FR and 116 RF)
304 of DNA motif sequences showed a significantly higher ratio of EPI predicted based on
305 EPA (i) overlapped with the chromatin interactions than EPI predicted based on EPA
306 (iii) (Table 4; Supplemental material 2). The difference between EPI predicted based on
307 EPA (i) and (ii) seemed to be difficult to distinguish using the chromatin interaction
308 data and the statistical test in some cases. However, as for the difference between EPI
309 predicted based on EPA (i) and (iii), a larger number of biased orientations of DNA
310 motif sequences was found to be correlated with chromatin interaction data. Chromatin
311 interaction data were obtained from different samples from DNase-seq, open chromatin
312 regions, so individual differences seemed to be large from the results of this analysis.
313 Most of biased orientations of DNA motif sequences (97%) were found to be correlated
314 with chromatin interactions, when comparing EPI predicted based on EPA (i) and (iii)
315 with HiChIP chromatin interactions.

316 Moreover, to examine the enhancer activity of EPI, the distribution of expression
317 level of putative target genes of EPI was compared between EPI overlapped with
318 HiChIP chromatin interactions and EPI not overlapped with them. Though the target

319 genes of EPI were selected from top 60% expression level of all transcripts (genes)
320 excluding transcripts not expressed in T cells, target genes of EPI overlapped with
321 chromatin interactions showed a significantly higher expression level than EPI not
322 overlapped with them, suggesting that EPI overlapped with chromatin interactions
323 activated the expression of target genes in T cells. All FR and RF orientations of DNA
324 motifs showed a significantly higher expression level of putative target genes of EPI
325 overlapped with chromatin interactions than EPI not overlapped. When a biased
326 orientation of DNA motif showed a significantly higher expression level of putative
327 target genes of EPI overlapped with chromatin interactions than EPI not overlapped, '1'
328 was marked with in the tables of the comparison between EPI and HiChIP chromatin
329 interactions in Supplemental material 2. When a DNA motif showed a significantly
330 lower expression level, '-1' was marked with, and when there was not significant
331 difference of expression level, '0' was marked with. However, they were not observed
332 in this analysis. HiChIP data were produced using H3K27ac antibody, so chromatin
333 interactions acting as repressor would not be identified.

334 The ratio of EPI overlapped with HiChIP chromatin interactions was also
335 increased using H3K27ac marks. Chromatin interaction data were obtained from
336 different samples from DNase-seq, open chromatin regions in $CD4^+$ T cells, so
337 individual differences seemed to exist from the results of this analysis, and (Mumbach
338 et al. 2017) suggested that individual differences of chromatin interactions were larger
339 than those of open chromatin regions. ATAC-seq data, open chromatin regions were
340 available in $CD4^+$ T cells in the paper, however, when using ATAC-seq data, the result

341 of the analysis of biased orientations of DNA motif sequences was different from
342 DNase-seq data, and not included a part of CTCF and cohesin. Thus, DNase-seq data
343 collected from ENCODE and Blueprint projects were employed in this study.
344

345 Discussion

346 To find DNA motif sequences of transcription factors (TF) and repeat DNA
347 sequences affecting the expression level of human putative transcriptional target genes,
348 the DNA motif sequences were searched from open chromatin regions of monocytes of
349 four people. Total 229 biased [130 forward-reverse (FR) and 128 reverse-forward (RF)]
350 orientation of DNA motif sequences of TF were found in monocytes of four people in
351 common, whereas only 11 any orientation (i.e. without considering orientation) of DNA
352 motif sequence of TF was found to affect the expression level of putative transcriptional
353 target genes, suggesting that enhancer-promoter association (EPA) shortened at the
354 genomic locations of FR or RF orientation of the DNA motif sequence of a TF or a
355 repeat DNA sequence is an important character for the prediction of enhancer-promoter
356 interactions (EPI) and the transcriptional regulation of genes.

357 When DNA motif sequences were searched from monocytes of one person, a
358 larger number of biased orientations of DNA motif sequences affecting the expression
359 level of human putative transcriptional target genes were found. When the number of
360 donors, from which experimental data were obtained, was increased, the number of
361 DNA motif sequences found in all people in common decreased and in some cases,
362 known transcription factors involved in chromatin interactions such as CTCF and

363 cohesin (RAD21 and SMC3) were not identified by statistical tests. This would be
364 caused by individual difference of the same cell type, low quality of experimental data,
365 and experimental errors. Moreover, though FR orientation of DNA binding motif
366 sequences of CTCF and cohesin is frequently observed at chromatin interaction anchors,
367 the percentage of FR orientation is not 100, and other orientations of the DNA binding
368 motif sequences are also observed (Guo et al. 2015). Though DNA binding motif
369 sequences of CTCF and cohesin are found in various open chromatin regions, DNA
370 binding motif sequences of some TF would be observed less frequently in open
371 chromatin regions. The analyses of experimental data of a number of people would
372 avoid missing relatively weak statistical significance of DNA motif sequences of TF in
373 experimental data of each person by multiple testing correction of thousands of
374 statistical tests. A DNA motif sequence was found with p-value < 0.05 in experimental
375 data of one person and the DNA motif sequence found in the same cell type of four
376 people in common would have p-value < $0.05^4 = 6.25 \times 10^{-6}$. Actually, DNA motif
377 sequences with p-value slightly less than 0.05 in monocytes of one person were
378 observed in monocytes of four people in common.

379 At first, EPI were compared with chromatin interactions (Hi-C) in monocytes.
380 Using open chromatin regions overlapped with ChIP-seq experimental data of histone
381 modification of an enhancer mark (H3K27ac), the ratio of EPI not overlapped with
382 Hi-C was reduced. (Phanstiel et al. 2017) also reported that there was an especially
383 strong enrichment for loops with H3K27 acetylation peaks at both ends (Fisher's Exact
384 Test, $p = 1.4 \times 10^{-27}$). However, the total number of EPI overlapped with chromatin

385 interactions was also reduced using H3K27ac peaks, so more chromatin interaction data
386 would be needed to obtain reliable results in this analysis. As an issue of experimental
387 data, data for chromatin interactions and open chromatin regions were obtained from
388 different samples and donors, so individual differences would exist in the data. The
389 resolution of chromatin interaction data used in monocytes was about 50kb, thus the
390 number of chromatin interactions was relatively small (72,284 at 50kb resolution with a
391 cutoff score of CHiCAGO tool > 1 and 16,501 with a cutoff score of CHiCAGO tool >
392 5) ('PCHiC_peak_matrix_cutoff0.txt.gz' file was downloaded from 'Promoter Capture
393 Hi-C in 17 human primary blood cell types' website https://osf.io/u8tzp/files/). To
394 examine the difference of the numbers of EPI overlapped with chromatin interactions,
395 according to the three types of EPAs, the number of chromatin interactions should be
396 large enough.

397 As HiChIP chromatin interaction data were available in $CD4^+$ T cells, biased
398 orientations of DNA motif sequences of TF were examined in T cells using DNase-seq
399 data of four people. The resolutions of chromatin interactions and EPI were adjusted to
400 5kb by fragmentation of genome sequences. The number of HiChIP chromatin
401 interactions was 19,926,360 at 5kb resolution, 666,149 at 5kb resolution with chromatin
402 interactions (more than 1,000 counts for each interaction), and 78,209 at 5kb resolution
403 with chromatin interactions (more than 6,000 counts for each interaction). As expected,
404 the number of EPI overlapped with chromatin interactions was increased, and 51 – 204
405 of biased orientations of DNA motif sequences of TF showed a statistical significance
406 in EPI predicted based on EPA shortened at the genomic locations of the DNA motif

407 sequence, compared with the other types of EPAs or EPA not shortened. False positive
408 prediction of EPI would be reduced by using H3K27ac marks and other features. The
409 ratio of EPI overlapped with HiChIP chromatin interactions was increased using
410 H3K27ac marks. However, the number of biased orientations of DNA motif sequences
411 showing a higher ratio of EPI overlapped with HiChIP chromatin interactions than the
412 other types of EPAs was decreased using H3K27ac marks (Supplemental material 2).
413 HiChIP analysis used H3K27ac antibody to capture chromatin interactions and
414 identified twenty millions of chromatin interactions, but the number of peaks of
415 ChIP-seq data of H3K27ac is usually less than a hundred thousand. There seems to be
416 much difference of the number of H3K27ac sites between HiChIP and ChIP-seq, so
417 ChIP-seq of H3K27ac may not cover all H3K27ac sites.

418 When forming a homodimer or heterodimer with another TF, TF may bind to
419 genome DNA with a specific orientation of their DNA binding sequences (Fig. 3). From
420 the analysis of biased orientations of DNA motif sequences of TF, TF forming
421 heterodimer would also be found. If the DNA binding motif sequence of only the mate
422 to a pair of TF was found in EPA, EPA was shortened at one side, which is the genomic
423 location of the DNA binding motif sequence of the mate to the pair, and transcriptional
424 target genes were predicted using the EPA shortened at the side. In this analysis, the
425 mate to both heterodimer and homodimer of TF can be used to examine the effect on
426 the expression level of transcriptional target genes predicted based on the EPA
427 shortened at one side. For heterodimer, biased orientations of DNA motif sequences
428 may also be found in forward-forward or reverse-reverse orientation.

429 In general, DNA motif sequences of TF were searched from genome sequences
430 using position weight matrix or position frequency matrix and allowing substitution of
431 DNA sequences under a certain threshold. However, the change of the threshold
432 affected the result of analyses and it seems to be difficult to find the best parameter
433 setting to reduce false-positive and false-negative predictions of DNA biding sites of TF.
434 Therefore, to obtain a robust result in this study, position weight matrixes of DNA
435 motifs were converted into consensus DNA sequences including degenerated sites,
436 which consist of A, T, G, C, R, Y, M, K, S, W, B, H, V, D, and N letters. This does not
437 need parameter setting in the search for DNA motif sequences, and is the same as *k*-mer
438 analysis of DNA motif sequences of TF. Thought the number of genomic regions
439 matched with a DNA motif sequence was decreased, about 200 FR and RF orientations
440 of DNA motif sequences of TF were found, and the number of any orientation of DNA
441 motif sequences was quite small. Though the number of biased orientations of DNA
442 motif sequences of TF was decreased, the number of the DNA motif sequences found in
443 both monocytes and $CD4^+$ T cells in common was increased, suggesting that
444 false-positive prediction of DNA biding sites of TF was reduced. However, the length
445 of the consensus DNA sequences of some TF is relatively long. When the core DNA
446 binding sequence of a TF is short (5 or 6 bp), it may be strict to find perfect matches of
447 the long consensus DNA sequence in genome sequences, not allowing a substitution of
448 a DNA sequence. To obtain more accurate result of analysis, I plan to refine the method
449 to find biased orientations of DNA motif sequences of TF.
450 It has been reported that CTCF and cohesin-binding sites are frequently mutated

451 in cancer (Katainen et al. 2015). Some biased orientations of DNA motif sequences
452 would be associated with chromatin interactions and might be associated with diseases
453 including cancer.

454 The analyses in this study revealed novel characters of DNA binding motif
455 sequences of TF and repeat DNA sequences to analyze TF involved in chromatin
456 interactions, insulator function and forming a homodimer, heterodimer or complex with
457 other TF, affecting the transcriptional regulation of genes.

458

459 ## Methods

460 **Search for biased orientations of DNA motif sequences**

461 To examine transcriptional regulatory target genes of transcription factors (TF),
462 bed files of hg38 of Blueprint DNase-seq data for $CD14^+$ monocytes of four donors
463 (EGAD00001002286; Donor ID: C0010K, C0011I, C001UY, C00408) were obtained
464 from Blueprint project web site (http://dcc.blueprint-epigenome.eu/#/home), and the bed
465 files of hg38 were converted into those of hg19 using Batch Coordinate Conversion
466 (liftOver) web site (https://genome.ucsc.edu/util.html).

467 As high resolution of chromatin interaction data using HiChIP became available
468 in $CD4^+$ T cells, to promote the same analysis of $CD14^+$ monocytes in $CD4^+$ T cells,
469 DNase-seq data of four donors were obtained from a public database and Blueprint
470 projects web sites. DNase-seq data of only one donor was available in Blueprint project
471 for $CD4^+$ T cells (Donor ID: S008H1), and three other DNase-seq data were obtained
472 from NCBI Gene Expression Omnibus (GEO) database. Though the peak calling of

473 DNase-seq data available in GEO database was different from other DNase-seq data in
474 ENCODE and Blueprint projects where 150bp length of peaks were usually predicted
475 using HotSpot (John et al. 2011), FASTQ files of DNase-seq data were downloaded
476 from NCBI Sequence Read Archive (SRA) database (SRR097566, SRR097618, and
477 SRR171574). Read sequences of the FASTQ files were aligned to the hg19 version of
478 the human genome reference using BWA (Li and Durbin 2009), and the BAM files
479 generated by BWA were converted into SAM files, sorted, and indexed using Samtools
480 (Li et al. 2009). Peaks of the DNase-seq data were predicted using HotSpot-4.1.1.

481 To identify transcription factor binding sites (TFBS) from the DNase-seq data,
482 TRANSFAC (2019.2), JASPAR (2018), UniPROBE (2018), high-throughput SELEX,
483 transcription factor binding sequences of ENCODE ChIP-seq data, and HOCOMOCO
484 version 9 and 11 were used to predict insulator sites (Wingender et al. 1996; Newburger
485 and Bulyk 2009; Portales-Casamar et al. 2010; Xie et al. 2010; Zhao and Stormo 2011;
486 Jolma et al. 2013; Kheradpour and Kellis 2014; Kulakovskiy et al. 2018). TRANSFAC
487 (2019.2) was used to analyze enhancer-promoter interactions, since these data were
488 sufficient to identify biased orientations of DNA motif sequences of TF with less
489 computational time, reducing the number of any orientation of DNA motif sequences of
490 TF. Position weight matrices of transcription factor binding sequences were converted
491 into DNA consensus sequences considering degenerated sites using convert matrix in
492 RSAT website (van Helden 2003). Transcription factor binding sequences of TF
493 derived from vertebrates were used for further analyses. Transcription factor binding
494 sequences were searched from each narrow peak of DNase-seq data in repeat-masked

495 hg19 genome sequences using Match tool in TRANSFAC with similarity score cutoff
496 of 1 after transforming the DNA consensus sequences of TF into position frequency
497 matrixes for Match search (Kel et al. 2003). Repeat-masked hg19 genome sequences
498 were downloaded from UCSC genome browser (http://genome.ucsc.edu/,
499 http://hgdownload.soe.ucsc.edu/goldenPath/hg19/bigZips/hg19.fa.masked.gz). TF
500 corresponding to transcription factor binding sequences were searched computationally
501 and manually by comparing their names and gene symbols of HGNC (HUGO Gene
502 Nomenclature Committee) -approved gene nomenclature and 31,848 UCSC known
503 canonical transcripts
504 (http://hgdownload.soe.ucsc.edu/goldenPath/hg19/database/knownCanonical.txt.gz), as
505 transcription factor binding sequences were not linked to transcript IDs such as UCSC,
506 RefSeq, and Ensembl transcripts.

507 Target genes of a TF were assigned when its TFBS was found in DNase-seq
508 narrow peaks in promoter or extended regions for enhancer-promoter association of
509 genes (EPA). Promoter and extended regions were defined as follows: promoter regions
510 were those that were within distance of ±5 kb from transcriptional start sites (TSS).
511 Promoter and extended regions were defined as per the following association rule,
512 which is the same as that defined in Figure 3A of a previous study (McLean et al.
513 2010): the single nearest gene association rule, which extends the regulatory domain to
514 the midpoint between the TSS of the gene and that of the nearest gene upstream and
515 downstream without the limitation of extension length. Extended regions for EPA were
516 shortened at the genomic locations of DNA binding sites of a TF that was the closest to

517 a transcriptional start site, and transcriptional target genes were predicted from the
518 shortened enhancer regions using TFBS. Furthermore, promoter and extended regions
519 for EPA were shortened at the genomic locations of forward–reverse (FR) orientation of
520 DNA binding sites of a TF. When forward or reverse orientation of DNA binding sites
521 were continuously located in genome sequences several times, the most external
522 forward–reverse orientation of DNA binding sites were selected. The genomic positions
523 of genes were identified using 'knownGene.txt.gz' file in UCSC bioinformatics sites
524 (Karolchik et al. 2014). The file 'knownCanonical.txt.gz' was also utilized for choosing
525 representative transcripts among various alternate forms for assigning promoter and
526 extended regions for EPA. From the list of transcription factor binding sequences and
527 transcriptional target genes, redundant transcription factor binding sequences were
528 removed by comparing the target genes of a transcription factor binding sequence and
529 its corresponding TF; if identical, one of the transcription factor binding sequences was
530 used. When the number of transcriptional target genes predicted from a transcription
531 factor binding sequence was less than five, the transcription factor binding sequence
532 was omitted.

533 Repeat DNA sequences were searched from the hg19 version of the human
534 reference genome using RepeatMasker (Smit, AFA & Green, P RepeatMasker at
535 http://www.repeatmasker.org) and RepBase RepeatMasker Edition
536 (http://www.girinst.org).

537 For gene expression data, RNA-seq reads mapped onto human hg19 genome
538 sequences were obtained from UCSF-UBC human reference epigenome mapping

539 project RNA-seq reads with poly-A of naive $CD4^+$ T cells (GSM669617). FPKMs of
540 the RNA-seq data were calculated using RSeQC (Wang et al. 2012). For monocytes,
541 Blueprint RNA-seq FPKM data
542 ('C0010KB1.transcript_quantification.rsem_grape2_crg.GRCh38.20150622.results',
543 'C0011IB1.transcript_quantification.rsem_grape2_crg.GRCh38.20150622.results', and
544 'C001UYB4.transcript_quantification.rsem_grape2_crg.GRCh38.20150622.results')
545 were downloaded from Blueprint DCC portal
546 (http://dcc.blueprint-epigenome.eu/#/files). However, RNA-seq FPKM data for C00408
547 was not available, so RNA-seq FPKM data for C001UY was used for C00408. Based
548 on FPKM, UCSC transcripts were arranged in descending order of expression level, and
549 top 4,000 transcripts were selected in each cell type.

550 The expression level of transcriptional target genes predicted based on EPA
551 shortened at the genomic locations of DNA motif sequence of a TF or a repeat DNA
552 sequence was compared with the expression level of transcriptional target genes
553 predicted from promoter. For each DNA motif sequence shortening EPA,
554 transcriptional target genes were predicted using about 3,000 – 5,000 DNA binding
555 motif sequences of TF, and the distribution of expression level of putative
556 transcriptional target genes of each TF was compared between EPA and only promoter
557 using Mann-Whitney test, two-sided (p-value < 0.05). The number of TF showing a
558 significant difference of expression level of putative transcriptional target genes
559 between EPA and promoter was compared among forward-reverse (FR),
560 reverse-forward (RF), and any orientation (i.e. without considering orientation) of a

561 DNA motif sequence shortening EPA using Fisher's exact test (p-value < 0.05). When a
562 DNA motif sequence of a TF or a repeat DNA sequence shortening EPA showed a
563 significant difference of expression level of putative transcriptional target genes among
564 FR, RF, or any orientation in monocytes of four people in common, the DNA motif
565 sequence was listed.

566 Though forward-reverse orientation of DNA binding motif sequences of CTCF
567 and cohesin are frequently observed at chromatin interaction anchors, the percentage of
568 forward-reverse orientation is not 100, and other orientations of the DNA binding motif
569 sequences are also observed (Guo et al. 2015). Though DNA binding motif sequences
570 of CTCF and cohesin are found in various open chromatin regions, DNA binding motif
571 sequences of some transcription factors would be observed less frequently in open
572 chromatin regions. The analyses of experimental data of a number of people would
573 avoid missing relatively weak statistical significance of DNA motif sequences in
574 experimental data of each person by multiple testing correction of thousands of
575 statistical tests. A DNA motif sequence was found with p-value < 0.05 in experimental
576 data of one person and the DNA motif sequence found in the same cell type of four
577 people in common would have p-value $< 0.05^4 = 6.25 \times 10^{-6}$.

578

579 **Co-location of biased orientations of DNA motif sequences**

580 Co-location of biased orientations of DNA binding motif sequences of TF was
581 examined. The number of open chromatin regions with the same pair of DNA binding
582 motif sequences was counted, and when the pair of DNA binding motif sequences were

583 enriched with statistical significance (Fisher's exact test, p-value $< 1.0 \times 10^{-9}$), they
584 were listed.
585
586 **Comparison with chromatin interaction data**
587 For comparison of EPA with chromatin interactions (HiChIP) in $CD4^+$ T cells,
588 'GSM2705049_Naive_HiChIP_H3K27ac_B2T1_allValidPairs.txt',
589 'GSM2705050_Naive_HiChIP_H3K27ac_B2T2_allValidPairs.txt', and
590 'GSM2705051_Naive_HiChIP_H3K27ac_B3T1_allValidPairs.txt' files were
591 downloaded from Gene Expression Omnibus (GEO) database (GSM2705049,
592 GSM2705050 and GSM2705051). The resolutions of chromatin interaction data and
593 EPI were adjusted to 5kb before their comparison. Chromatin interactions with more
594 than 6,000 and 1,000 counts for each interaction were used in this study.
595 Enhancer-promoter interactions (EPI) were predicted using three types of EPAs
596 in monocytes: (i) EPA shortened at the genomic locations of FR or RF orientation of
597 DNA motif sequence of a TF, (ii) EPA shortened at the genomic locations of any
598 orientation (i.e. without considering orientation) of DNA motif sequence of a TF, and
599 (iii) EPA without being shortened by a DNA motif sequence. EPI predicted using the
600 three types of EPAs in common were removed. First, EPI predicted based on EPA (i)
601 were compared with chromatin interactions. The resolution of chromatin interaction
602 data used in this study was 1-5kb, so EPI were adjusted to 5kb before their comparison.
603 The number and ratio of EPI overlapped with chromatin interactions were counted.
604 Second, EPI were predicted based on EPA (ii), and EPI predicted based on EPA (i)

605 were removed from the EPI. The number and ratio of EPI overlapped with chromatin
606 interactions were counted. Third, EPI were predicted based on EPA (iii), and EPI
607 predicted based on EPA (i) and (ii) were removed from the EPI. The number and ratio
608 of EPI overlapped with chromatin interactions were counted. The number and ratio of
609 the EPI were compared two times between EPA (i) and (iii), and EPA (i) and (ii)
610 (binomial distribution, p-value < 0.025 for each test, two-sided, 95% confidence
611 interval).

612 Putative target genes for the analysis of EPI were selected from top 50%
613 expression level of all transcripts excluding transcripts not expressed in monocytes and
614 top 60% expression level of transcripts in $CD4^+$ T cells. The expression level of putative
615 target genes of EPI overlapped with HiChIP chromatin interactions was compared with
616 EPI not overlapped with them. For each FR or RF orientation of DNA motif, EPI were
617 predicted based on EPA and the overlap of EPI with chromatin interactions was
618 examined. When a putative transcriptional target gene of a TF in an enhancer was found
619 in both EPI overlapped with a chromatin interaction and EPI not overlapped with, the
620 target gene was removed. The distribution of expression level of putative target genes
621 was compared using Mann-Whitney test, two-sided (p-value < 0.05).

622

623 **Acknowledgements**

624 The supercomputing resource was provided by Human Genome Center of the Institute
625 of Medical Science at the University of Tokyo. Computations were partially performed
626 on the NIG supercomputer at ROIS National Institute of Genetics. Publication charges

627 for this article were funded by JSPS KAKENHI Grant Number 16K00387. This
628 research was partially supported by the Platform Project for Supporting in Drug
629 Discovery and Life Science Research（Platform for Dynamic Approaches to Living
630 System）from Japan Agency for Medical Research and Development (AMED). This
631 research was partially supported by Development of Fundamental Technologies for
632 Diagnosis and Therapy Based upon Epigenome Analysis from Japan Agency for
633 Medical Research and Development (AMED). This work was partially supported by
634 JST CREST Grant Number JPMJCR15G1, Japan.
635

636 **Figures**

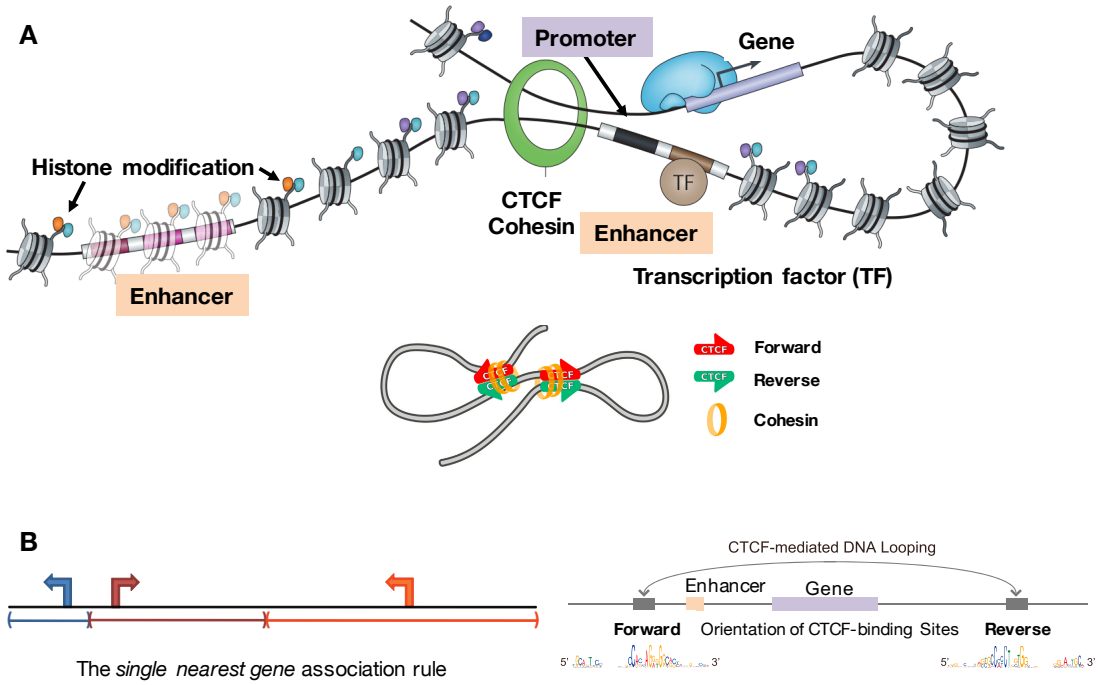

637

638 **Figure 1.** Chromatin interactions and enhancer-promoter association. (A) Forward–
639 reverse orientation of CTCF-binding sites are frequently found in chromatin interaction
640 anchors. CTCF can block the interaction between enhancers and promoters limiting the
641 activity of enhancers to certain functional domains (de Wit et al. 2015; Guo et al. 2015).
642 (B) Computationally-defined regulatory domains for enhancer-promoter association
643 (McLean et al. 2010). The *single nearest gene* association rule extends the regulatory
644 domain to the midpoint between this gene's TSS and the nearest gene's TSS both
645 upstream and downstream. Enhancer-promoter association was shortened at the
646 genomic locations of forward-reverse orientation of DNA binding motif sequence of a
647 transcription factor (e.g. CTCF in the figure).

648

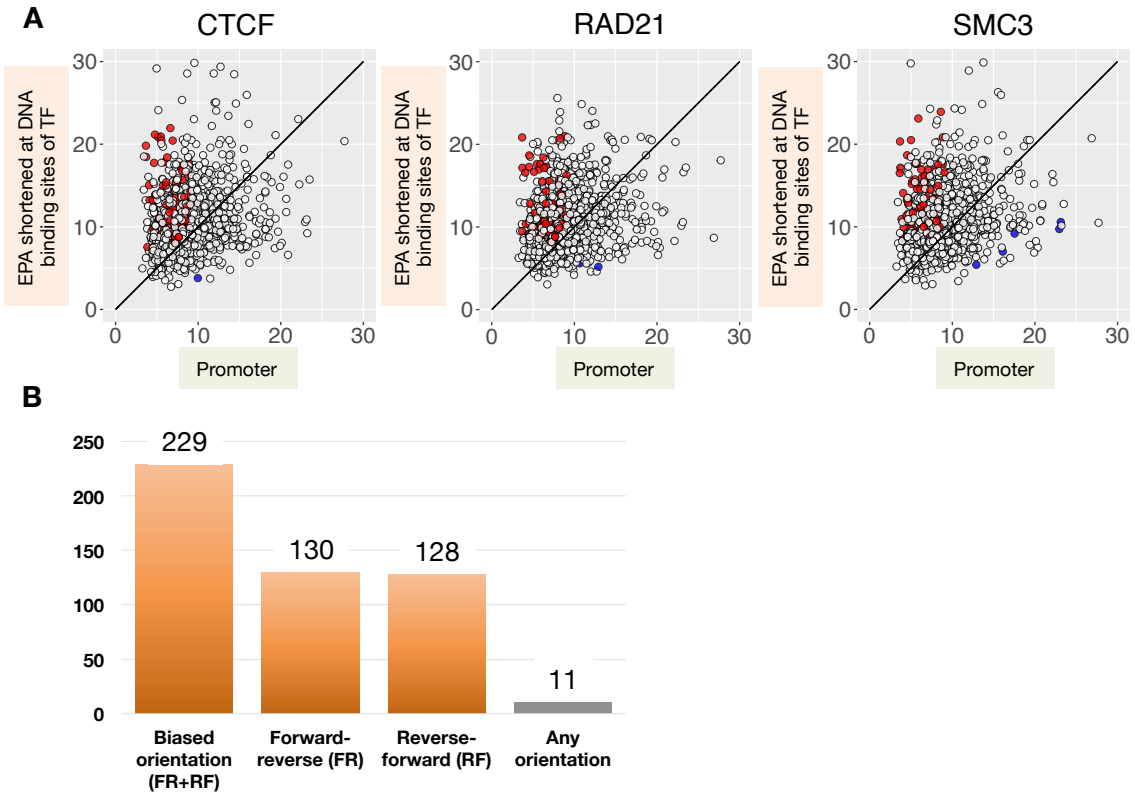

Figure 2. Biased orientations of DNA motif sequences of transcription factors affecting the transcription of genes. (A) Comparison of expression level of putative transcriptional target genes. The median expression levels of target genes of the same transcription factor binding sequences were compared between promoters and enhancer-promoter association (EPA) shortened at the genomic locations of forward-reverse orientation of DNA motif sequence of CTCF and cohesin (RAD21 and SMC3) respectively in monocytes. Red and blue dots show statistically significant difference (Mann-Whitney test) of the distribution of expression levels of target genes between promoters and the EPA. Red dots show the median expression level of target genes was higher based on the EPA than promoters, and blue dots show the median expression level of target genes was lower based on the EPA than promoters. The

661 expression level of target genes predicted based on the EPA tended to be higher than
662 promoters, implying that transcription factors acted as activators of target genes. (B)
663 Biased orientations of DNA motif sequences of transcription factors in monocytes.
664 Total 229 of biased orientations of DNA binding motif sequences of transcription
665 factors were found to affect the expression level of putative transcriptional target genes
666 in monocytes of four people in common, whereas only 11 any orientation (i.e. without
667 considering orientation) of DNA binding motif sequence was found to affect the
668 expression level.
669

670

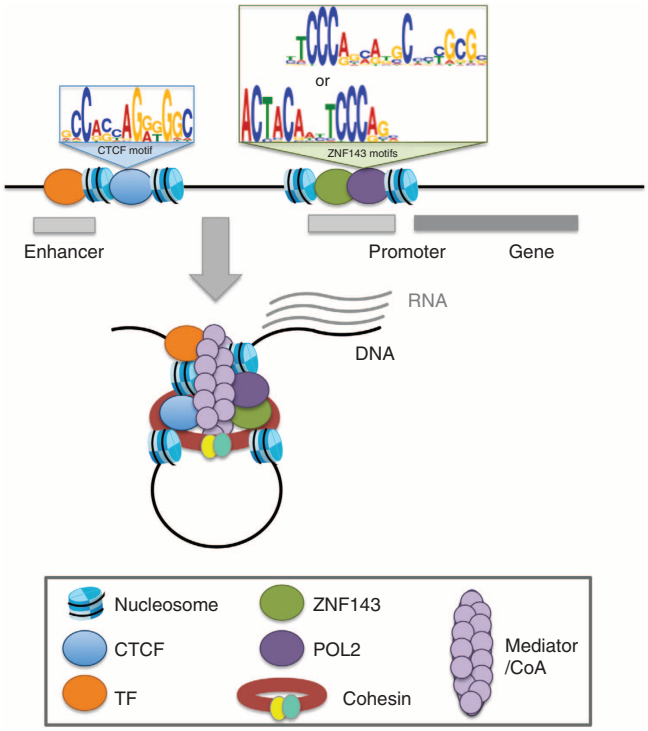

671

672 **Figure 3.** Schematic representation of chromatin interactions involving gene promoters.

673 ZNF143 contributes the formation of chromatin interactions by directly binding the

674 promoter of genes establishing looping with distal element bound by CTCF (Bailey et al.

675 2015).

676

677 **Tables**

678 **Table 1.** Top 90 biased orientations of DNA binding motif sequences of transcription

679 factors in monocytes. TF: DNA binding motif sequences of transcription factors. Score:

680 $-\log_{10}$ (*p*-value).

681 Forward-reverse orientation

TF	Score	TF	Score	TF	Score
TCF3	123.12	ETS	49.44	DDIT3	29.23
ZNF592	120.55	SOX6	49.42	NRF1	28.86
EOMES	109.78	AP2A	49.36	SREBP2	28.63
GMEB2	75.32	CEBPA	47.31	YY1	28.02
CEBPG	74.27	FOSL1	44.41	FOXM1	27.64
FOXA1	73.14	ATOH1	43.94	VSX1	27.38
FOXA2	72.93	NFATC2	43.63	AP-1	27.13
DBX2	72.66	TBX3	42.82	STAT5A	26.61
NFYA	71.62	CREB	42.45	KLF10	26.24
TP53	66.60	EGR1	41.57	mix-a	26.06
E2F4	65.71	HOXA4	41.47	HLF	25.64
TLX2	64.10	FOXO1	40.92	FOXG1	25.44
IKZF1	63.69	BARHL1	40.43	DLX3	24.92
RFX6	61.62	ZNF189	39.78	ZNF180	24.86
SFN	59.89	SP1	39.54	BARX2	24.45
FOXO3	59.78	ATF3	37.30	REST	24.25
ZBTB18	59.45	CTNNB1	37.01	SMAD	24.05
PPARG	57.25	ZNF579	36.10	RAD21	23.98
ZNF675	54.71	MZF1	35.58	SRY	23.97
HNF1B	53.86	BACH2	35.38	LRF	23.46
ITGB2	53.86	ZIC1	34.59	ZNF300	22.62
RFX4	53.41	CTCFL	34.55	FOXJ2	22.35
TBP	53.06	CXXC1	34.42	TCF7	22.18
CBFB	52.31	GCM2	34.26	MNX1	21.99
TEAD1	51.39	MEIS1:EOMES	34.02	SOX	21.98
ZBTB7A	50.61	HNF4	34.00	MAZ	21.87
CTCF	50.54	HINFP	33.29	HMGIY	21.53
SOX5	50.51	PDX1	32.36	STAT4	21.33
BRCA1	50.47	CEBPD	30.87	TBR1	21.22
SOX3	49.47	RUNX1	29.40	NKX2-5	21.17

682
683

Reverse-forward orientation

TF	Score	TF	Score	TF	Score
ZBTB48	175.35	HOXA11	47.37	CEBP	32.34
ZBTB38	107.55	POU4F3	46.76	RUNX3	32.09
MSX1	105.86	LBX1	46.13	TCF7	31.09
POLYA	98.31	NR5A1	44.93	AR	30.08
RFX5	97.45	ETV5	44.91	ZBTB7B	29.59
SMAD1	83.39	FOXL1	44.50	ESX1	29.45
YBX1	80.34	NFATC2	43.63	CTNNB1	29.43
KLF4	79.72	NR3C1	42.45	HDAC2	29.27
NR2C2	78.27	ETV6	41.44	HIC1	29.16
OTX	74.43	TFAP2A	40.97	NRF1	29.02
CEBPG	74.27	TCF7L2	40.86	HOXD3	28.50
SP1	73.86	PGR	40.58	ZFP42	28.20
BARHL1	72.65	SP2	39.15	NR4A1	27.71
PITX3	71.71	EBF1	38.13	NR4A3	25.50
TEAD3	68.36	ZNF384	37.81	LMX1A	25.31
FOXA2	68.31	ISX	37.47	NFATC4	25.26
ZBTB16	68.09	GFI1	36.99	PAX2	25.04
EN2	64.71	ATF6	36.81	RAX2	24.73
HOXA7	64.52	REST	36.52	FOXD2	24.55
ZBTB7A	63.80	NFYB	36.38	RHOXF1	23.71
NFATC1	61.71	FOS	36.12	CTCFL	23.46
KLF2	61.64	RUNX2	35.21	CREB1	23.28
TEAD1	61.03	YY1	34.76	EN1	22.00
STAT	56.11	CREB3	34.64	SPIB	21.81
SOX6	55.25	MEIS1	34.49	NFAT	20.97
TFAP2C	53.06	CTCF	33.99	LEF1	20.94
HOXA2	52.05	EGR1	33.22	MYB	20.77
FOXO4	51.30	ISL2	33.21	NKX3-2	20.72
ZBTB18	49.30	RUNX1	33.17	CCAAT	20.42
SPDEF	49.26	PDX1	32.57	FLI1	19.65

Table 2. Biased orientation of repeat DNA sequences in monocytes. Score: $-\log_{10}$ (*p*-value).

Reverse-forward (RF) orient

Repeat DNA seq.	Score
AluJo	85.18
AluJb	17.73
L1M5	12.24

Reverse-forward (RF) orientation (using H3K27ac histone modification marks)

Repeat DNA seq.	Score
AluJb	26.27

Table 3. Top 30 of co-locations of biased orientations of DNA binding motif sequences of transcription factors in monocytes. Co-locations of DNA motif sequence of CTCF with another biased orientation of DNA motif sequence were shown in a separate table. Motif 1,2: DNA binding motif sequences of transcription factors. # both: the number of open chromatin regions including both Motif 1 and Motif 2. # motif 1: the number of open chromatin regions including Motif 1. # motif 2: the number of open chromatin regions including Motif 2. # others: the number of open chromatin regions not including Motif 1 and Motif 2. Total number of open chromatin regions is 145,866.

Motif 1	Motif 2	# both	# motif 1	# motif 2	# others	p-value
SOX	TCF7L2	21268	0	129	124469	0
LEF1	TCF7L2	21268	0	126	124472	0
LEF1	SOX	21268	129	126	124343	0
DLX5	PRRX2	20580	0	128	125158	0
NFAT	NFATC4	16105	0	110	129651	0
ETV4	FLI1	15046	3276	0	127544	0
LEF1	SOX10	14773	24783	6621	99689	0
SOX	SOX10	14772	24784	6625	99685	0
SOX10	TCF7L2	14744	6524	24812	99786	0
ELF5	ETV4	13205	5117	6384	121160	0
ELF5	FLI1	12971	6618	2075	124202	0
RUNX2	RUNX3	12875	3088	174	129729	0
RUNX1	RUNX3	12866	0	183	132817	0
RUNX1	RUNX2	12866	3097	0	129903	0
HMGA1	HMX1	12611	0	15149	118106	0
NFATC1	NFATC3	10877	231	0	134758	0
NFATC1	NFATC4	10831	5274	277	129484	0
NFAT	NFATC1	10831	277	5384	129374	0
NFAT	NFATC3	10815	62	5400	129589	0
NFATC3	NFATC4	10815	5290	62	129699	0
BHLHE40	MITF	10319	65	19796	115686	0
HOXA2	MEOX2	9999	0	125	135742	0
EMX1	MEOX2	9999	0	125	135742	0
BCL6	HMGA1	7648	4963	32936	100319	0
MEIS1	MEIS3	6973	4122	13183	121588	0
BHLHE40	TCF12	6343	23772	57	115694	0
HMGA1	STAT5A	4835	34254	2003	104774	0
FOXD2	FOXL1	4606	0	6432	134828	0
DLX3	DLX5	4561	24	16147	125134	0
DLX5	MSX1	4561	24	16147	125134	0

Motif 1	Motif 2	# both	# motif 1	# motif 2	# others	p-value
CTCF	RAD21	1450	0	1306	143110	0
CTCF	CTCFL	1061	389	399	144017	0
CTCF	ZBTB7A	634	14	7766	137452	0
CTCF	ZBTB7	633	517	15	144701	0
CTCF	ZNF300	505	8862	143	136356	0
CTCFL	RAD21	1459	1	1297	143109	0
CTCFL	ZBTB7A	1150	0	7250	137466	0
CTCFL	ZNF300	900	250	8467	136249	0
BHLHE40	CTCF	606	389	29509	115362	8.06E-169

719 **Table 4.** Comparison of enhancer-promoter interactions (EPI) with chromatin
720 interactions in T cells. The upper tables show the number of biased orientations of DNA
721 motifs, where a significantly higher ratio of EPI, which were predicted based on
722 enhancer-promoter association (EPA) (iii), overlapped with HiChIP chromatin
723 interaction data than the other types of EPA (i) and (ii). The middle tables show the 33
724 FR and 23 RF orientations of DNA motifs found in common among B2T1, B2T2 and
725 B3T1 replications in the upper table. The lower table shows that among 69 biased
726 orientations of DNA motifs found in both monocytes and T cell, 24 were matched with
727 the analysis of HiChIP for three types of EPA. TF: DNA binding motif sequence of a
728 transcription factor. Score: $-\log_{10}$ (*p*-value). Inf: *p*-value = 0. Score 1: Comparison of
729 EPA shortened at the genomic locations of FR or RF orientation of DNA motif
730 sequence [EPA (iii)] with EPA not shortened [EPA (i)]. Score 2: Comparison of EPA
731 shortened at the genomic locations of FR or RF orientation of DNA motif sequence
732 [EPA (iii)] with EPA shortened at the genomic locations of any orientation of DNA
733 motif sequence [EPA (ii)].

1. Comparison of EPI with HiChIP data among three EPA (i), (ii) and (iii)

Replication of HiChIP data	Total no. (FR + RF) of DNA motifs	No. of FR DNA motifs	No. of RF DNA motifs
B2T1	71	42	34
B2T2	81	47	40
B3T1	94	55	47
DNA motifs found in common among replications			
B2T1 and B2T2	60	35	30
B2T1 and B3T1	59	38	26
B2T2 and B3T1	68	42	32
B2T1, B2T2 and B3T1	51	33	23

2. Comparison of EPI with HiChIP data between two EPA (i) and (iii)

Replication of HiChIP data	Total no. (FR + RF) of DNA motifs	No. of FR DNA motifs	No. of RF DNA motifs
B2T1	205	116	117
B2T2	205	116	117
B3T1	208	119	119
DNA motifs found in common among replications			
B2T1 and B2T2	204	116	116
B2T1 and B3T1	205	116	117
B2T2 and B3T1	204	116	116
B2T1, B2T2 and B3T1	204	116	116

Forward-reverse (FR)

TF	Score 1	Score 2
AP-1	81.68	15.19
AP2A	142.68	5.30
BPTF	59.08	3.31
CTCF	323.31	7.60
CTCFL	323.31	2.44
DBP	118.88	18.18
DLX3	30.22	4.12
ETS1	82.43	2.00
FOSB	79.38	14.49
FOSL1	42.29	7.04
IKZF1	83.93	8.70
JUN	39.30	5.81
JUNB	110.84	3.66
KLF4	37.29	15.02
KLF5	68.20	9.30
LBX1	154.16	2.69
NEUROD2	48.90	4.73
NFIL3	152.37	2.69
NKX2-2	198.62	2.31
NKX2-5	136.48	8.97
NR2F1	82.58	7.16
NR3C1	77.96	17.53
RAD21	53.81	7.70
RFX7	29.86	1.93
SMARCC1	39.89	6.15
SMC3	300.51	23.65
SPI1	219.80	7.68
SREBF2	68.43	2.84
TEAD4	45.79	10.37
VDR:RXRA	82.58	7.16
ZBTB7A	101.61	5.36
ZEB1	107.06	5.51
ZXDC	23.35	6.26

Reverse-forward (RF)

TF	Score 1	Score 2
AP-1	79.38	14.49
CACD	67.66	8.44
CRX	56.13	4.27
CTCF	5.65	3.43
CTCFL	101.61	5.36
ETV4	103.13	6.18
FOS	76.64	14.21
FOSL1	39.62	6.42
FOSL2	42.00	6.41
FOXA2	323.31	1.69
GATA	293.73	3.88
HDAC1	323.31	11.46
HEY2	257.47	3.23
HIC2	62.15	14.91
JUND:FOSL1	40.68	6.95
MEIS1	72.99	10.02
MEQ	118.91	5.86
NFI	101.48	10.50
NFIL3	114.14	2.15
SOX4	151.86	4.45
TFAP2C	136.94	5.62
YBX1	111.24	2.03
ZNF354C	54.72	6.02

Forward-reverse (FR)

TF	Score 1	Score 2
AP-1	81.68	15.19
AP2A	142.68	5.30
CTCF	323.31	7.60
CTCFL	323.31	2.44
DLX3	30.22	4.12
ETS1	82.43	2.00
FOSL1	42.29	7.04
IKZF1	83.93	8.70
JUN	39.30	5.81
KLF4	37.29	15.02
NKX2-5	136.48	8.97
RAD21	53.81	7.70
SPI1	219.80	7.68
ZBTB7A	101.61	5.36
ZEB1	107.06	5.51

Reverse-forward (RF)

TF	Score 1	Score 2
AP-1	79.38	14.49
CTCF	5.65	3.43
CTCFL	101.61	5.36
FOS	76.64	14.21
FOSL1	39.62	6.42
FOXA2	323.31	1.69
MEIS1	72.99	10.02
TFAP2C	136.94	5.62
YBX1	111.24	2.03

742 **References**

743

744 Bailey SD, Zhang X, Desai K, Aid M, Corradin O, Cowper-Sal Lari R, Akhtar-Zaidi B,
745 Scacheri PC, Haibe-Kains B, Lupien M. 2015. ZNF143 provides sequence
746 specificity to secure chromatin interactions at gene promoters. *Nat Commun* **2**:
747 6186.
748 Barutcu AR, Lajoie BR, Fritz AJ, McCord RP, Nickerson JA, van Wijnen AJ, Lian JB,
749 Stein JL, Dekker J, Stein GS et al. 2016. SMARCA4 regulates gene expression
750 and higher-order chromatin structure in proliferating mammary epithelial cells.
751 *Genome research* **26**: 1188-1201.
752 Bejerano G, Lowe CB, Ahituv N, King B, Siepel A, Salama SR, Rubin EM, Kent WJ,
753 Haussler D. 2006. A distal enhancer and an ultraconserved exon are derived
754 from a novel retroposon. *Nature* **441**: 87-90.
755 Chen M, Manley JL. 2009. Mechanisms of alternative splicing regulation: insights from
756 molecular and genomics approaches. *Nat Rev Mol Cell Biol* **10**: 741-754.
757 Das D, Clark TA, Schweitzer A, Yamamoto M, Marr H, Arribere J, Minovitsky S,
758 Poliakov A, Dubchak I, Blume JE et al. 2007. A correlation with exon
759 expression approach to identify cis-regulatory elements for tissue-specific
760 alternative splicing. *Nucleic acids research* **35**: 4845-4857.
761 de Souza FS, Franchini LF, Rubinstein M. 2013. Exaptation of transposable elements
762 into novel cis-regulatory elements: is the evidence always strong? *Mol Biol Evol*
763 **30**: 1239-1251.
764 de Wit E, Vos ES, Holwerda SJ, Valdes-Quezada C, Verstegen MJ, Teunissen H,
765 Splinter E, Wijchers PJ, Krijger PH, de Laat W. 2015. CTCF Binding Polarity
766 Determines Chromatin Looping. *Molecular cell* **60**: 676-684.
767 Gaussin A, Modlich U, Bauche C, Niederlander NJ, Schambach A, Duros C, Artus A,
768 Baum C, Cohen-Haguenauer O, Mermod N. 2012. CTF/NF1 transcription
769 factors act as potent genetic insulators for integrating gene transfer vectors.
770 *Gene Ther* **19**: 15-24.
771 Guo Y, Xu Q, Canzio D, Shou J, Li J, Gorkin DU, Jung I, Wu H, Zhai Y, Tang Y et al.
772 2015. CRISPR Inversion of CTCF Sites Alters Genome Topology and
773 Enhancer/Promoter Function. *Cell* **162**: 900-910.

774 Javierre BM, Burren OS, Wilder SP, Kreuzhuber R, Hill SM, Sewitz S, Cairns J,
775 Wingett SW, Varnai C, Thiecke MJ et al. 2016. Lineage-Specific Genome
776 Architecture Links Enhancers and Non-coding Disease Variants to Target Gene
777 Promoters. *Cell* **167**: 1369-1384 e1319.
778 Jeong M, Huang X, Zhang X, Su J, Shamim M, Bochkov I, Reyes J, Jung H, Heikamp
779 E, Presser Aiden A et al. 2017. A Cell Type-Specific Class of Chromatin Loops
780 Anchored at Large DNA Methylation Nadirs. *bioRxiv*.
781 Ji X, Dadon DB, Abraham BJ, Lee TI, Jaenisch R, Bradner JE, Young RA. 2015.
782 Chromatin proteomic profiling reveals novel proteins associated with
783 histone-marked genomic regions. *Proc Natl Acad Sci U S A* **112**: 3841-3846.
784 Jin C, Kato K, Chimura T, Yamasaki T, Nakade K, Murata T, Li H, Pan J, Zhao M, Sun
785 K et al. 2006. Regulation of histone acetylation and nucleosome assembly by
786 transcription factor JDP2. *Nat Struct Mol Biol* **13**: 331-338.
787 Jjingo D, Conley AB, Wang J, Marino-Ramirez L, Lunyak VV, Jordan IK. 2014.
788 Mammalian-wide interspersed repeat (MIR)-derived enhancers and the
789 regulation of human gene expression. *Mob DNA* **5**: 14.
790 John S, Sabo PJ, Thurman RE, Sung MH, Biddie SC, Johnson TA, Hager GL,
791 Stamatoyannopoulos JA. 2011. Chromatin accessibility pre-determines
792 glucocorticoid receptor binding patterns. *Nature genetics* **43**: 264-268.
793 Jolma A, Yan J, Whitington T, Toivonen J, Nitta KR, Rastas P, Morgunova E, Enge M,
794 Taipale M, Wei G et al. 2013. DNA-binding specificities of human transcription
795 factors. *Cell* **152**: 327-339.
796 Karolchik D, Barber GP, Casper J, Clawson H, Cline MS, Diekhans M, Dreszer TR,
797 Fujita PA, Guruvadoo L, Haeussler M et al. 2014. The UCSC Genome Browser
798 database: 2014 update. *Nucleic acids research* **42**: D764-770.
799 Katainen R, Dave K, Pitkanen E, Palin K, Kivioja T, Valimaki N, Gylfe AE,
800 Ristolainen H, Hanninen UA, Cajuso T et al. 2015. CTCF/cohesin-binding sites
801 are frequently mutated in cancer. *Nature genetics* **47**: 818-821.
802 Kel AE, Gossling E, Reuter I, Cheremushkin E, Kel-Margoulis OV, Wingender E. 2003.
803 MATCH: A tool for searching transcription factor binding sites in DNA
804 sequences. *Nucleic acids research* **31**: 3576-3579.
805 Kheradpour P, Kellis M. 2014. Systematic discovery and characterization of regulatory
806 motifs in ENCODE TF binding experiments. *Nucleic acids research* **42**:

807 2976-2987.
808 Kulakovskiy IV, Vorontsov IE, Yevshin IS, Sharipov RN, Fedorova AD, Rumynskiy EI,
809 Medvedeva YA, Magana-Mora A, Bajic VB, Papatsenko DA et al. 2018.
810 HOCOMOCO: towards a complete collection of transcription factor binding
811 models for human and mouse via large-scale ChIP-Seq analysis. *Nucleic acids*
812 *research* **46**: D252-D259.
813 Li H, Durbin R. 2009. Fast and accurate short read alignment with Burrows-Wheeler
814 transform. *Bioinformatics (Oxford, England)* **25**: 1754-1760.
815 Li H, Handsaker B, Wysoker A, Fennell T, Ruan J, Homer N, Marth G, Abecasis G,
816 Durbin R, Genome Project Data Processing S. 2009. The Sequence
817 Alignment/Map format and SAMtools. *Bioinformatics (Oxford, England)* **25**:
818 2078-2079.
819 McLean CY, Bristor D, Hiller M, Clarke SL, Schaar BT, Lowe CB, Wenger AM,
820 Bejerano G. 2010. GREAT improves functional interpretation of cis-regulatory
821 regions. *Nature biotechnology* **28**: 495-501.
822 Mumbach MR, Satpathy AT, Boyle EA, Dai C, Gowen BG, Cho SW, Nguyen ML,
823 Rubin AJ, Granja JM, Kazane KR et al. 2017. Enhancer connectome in primary
824 human cells identifies target genes of disease-associated DNA elements. *Nature*
825 *genetics* **49**: 1602-1612.
826 Newburger DE, Bulyk ML. 2009. UniPROBE: an online database of protein binding
827 microarray data on protein-DNA interactions. *Nucleic acids research* **37**:
828 D77-82.
829 Osato N. 2018. Characteristics of functional enrichment and gene expression level of
830 human putative transcriptional target genes. *BMC Genomics* **19**: 957.
831 Phanstiel DH, Van Bortle K, Spacek D, Hess GT, Shamim MS, Machol I, Love MI,
832 Aiden EL, Bassik MC, Snyder MP. 2017. Static and Dynamic DNA Loops form
833 AP-1-Bound Activation Hubs during Macrophage Development. *Molecular cell*
834 **67**: 1037-1048.e1036.
835 Portales-Casamar E, Thongjuea S, Kwon AT, Arenillas D, Zhao X, Valen E, Yusuf D,
836 Lenhard B, Wasserman WW, Sandelin A. 2010. JASPAR 2010: the greatly
837 expanded open-access database of transcription factor binding profiles. *Nucleic*
838 *acids research* **38**: D105-110.
839 Rebollo R, Romanish MT, Mager DL. 2012. Transposable elements: an abundant and

840 natural source of regulatory sequences for host genes. *Annu Rev Genet* **46**:
841 21-42.
842 Schreiber J, Libbrecht M, Bilmes J, Noble W. 2017. Nucleotide sequence and DNaseI
843 sensitivity are predictive of 3D chromatin architecture. *bioRxiv*.
844 Tabuchi TM, Deplancke B, Osato N, Zhu LJ, Barrasa MI, Harrison MM, Horvitz HR,
845 Walhout AJ, Hagstrom KA. 2011. Chromosome-biased binding and gene
846 regulation by the Caenorhabditis elegans DRM complex. *PLoS Genet* **7**:
847 e1002074.
848 van Helden J. 2003. Regulatory sequence analysis tools. *Nucleic acids research* **31**:
849 3593-3596.
850 Wang ET, Sandberg R, Luo S, Khrebtukova I, Zhang L, Mayr C, Kingsmore SF,
851 Schroth GP, Burge CB. 2008. Alternative isoform regulation in human tissue
852 transcriptomes. *Nature* **456**: 470-476.
853 Wang J, Vicente-Garcia C, Seruggia D, Molto E, Fernandez-Minan A, Neto A, Lee E,
854 Gomez-Skarmeta JL, Montoliu L, Lunyak VV et al. 2015. MIR retrotransposon
855 sequences provide insulators to the human genome. *Proc Natl Acad Sci U S A*
856 **112**: E4428-4437.
857 Wang L, Wang S, Li W. 2012. RSeQC: quality control of RNA-seq experiments.
858 *Bioinformatics (Oxford, England)* **28**: 2184-2185.
859 Weintraub AS, Li CH, Zamudio AV, Sigova AA, Hannett NM, Day DS, Abraham BJ,
860 Cohen MA, Nabet B, Buckley DL et al. 2017. YY1 Is a Structural Regulator of
861 Enhancer-Promoter Loops. *Cell* **171**: 1573-1588 e1528.
862 Wingender E, Dietze P, Karas H, Knuppel R. 1996. TRANSFAC: a database on
863 transcription factors and their DNA binding sites. *Nucleic acids research* **24**:
864 238-241.
865 Xie Z, Hu S, Blackshaw S, Zhu H, Qian J. 2010. hPDI: a database of experimental
866 human protein-DNA interactions. *Bioinformatics (Oxford, England)* **26**:
867 287-289.
868 Zhang H, Li F, Jia Y, Xu B, Zhang Y, Li X, Zhang Z. 2017. Characteristic arrangement
869 of nucleosomes is predictive of chromatin interactions at kilobase resolution.
870 *Nucleic acids research* **45**: 12739-12751.
871 Zhao Y, Stormo GD. 2011. Quantitative analysis demonstrates most transcription
872 factors require only simple models of specificity. *Nature biotechnology* **29**:

480-483.